ATP- and ADP-Dependent Modulation of RNA Unwinding and Strand Annealing Activities by the DEAD-Box Protein DED1[†]

Quansheng Yang and Eckhard Jankowsky*

Department of Biochemistry and Center for RNA Molecular Biology, School of Medicine, Case Western Reserve University, Cleveland, Ohio 44106

Received May 13, 2005; Revised Manuscript Received July 21, 2005

ABSTRACT: DEAD-box RNA helicases, which are involved in virtually all aspects of RNA metabolism, are generally viewed as enzymes that unwind RNA duplexes or disrupt RNA−protein interactions in an ATP-dependent manner. Here, we show in vitro that the DEAD-box protein DED1 from *Saccharomyces cerevisiae* promotes not only RNA unwinding but also strand annealing, the latter in such a profound fashion that the physical limit for a bimolecular association rate constant is approached. We further demonstrate that DED1 establishes an ATP-dependent steady state between unwinding and annealing, which enables the enzyme to modulate the balance between the two opposing activities through ATP and ADP concentrations. The ratio between unwinding and annealing and the degree to which both activities are ATP- and ADP-modulated are strongly influenced by structured as well as unstructured regions in the RNA substrate. Collectively, these findings expand the known functional repertoire of DEAD-box proteins and reveal the capacity of DED1 to remodel RNA in response to ADP and ATP concentrations by facilitating not only disruption but also formation of RNA duplexes.

Among the large number of diverse proteins that facilitate structural transitions of RNA in biological systems, the DExH/D proteins stand out, because of their ability to directly alter RNA structure in an ATP-dependent fashion (*1*). Members of the DExH/D protein family are involved in virtually all aspects of RNA metabolism, and these proteins represent the largest family of enzymes in eukaryotic RNA metabolism (*2*, *3*). DExH/D proteins contain at least eight characteristic sequence motifs that are conserved from bacteria to humans. The amino acid sequence of conserved motif II that often takes the form DEAD, DEAH, or DExH (combined DExH/D, in single letter code), provides the name for the protein family and for the three predominant subgroups, the DExH, the DEAH, and the DEAD-box proteins (*1*). DExH/D proteins are believed to catalyze many, if not all, ATP-driven[1] conformational changes in complexes that contain RNA, such as the spliceosome (*2*). Despite this central biological importance, the molecular mechanism(s) by which DExH/D proteins alter structure and/or composition of RNA−protein complexes remain poorly understood.

Many DExH/D proteins unwind RNA duplexes in vitro in an NTP-dependent fashion, and therefore, DExH/D proteins are frequently referred to as RNA helicases (*2*). Moreover, several DExH/D proteins have been shown to disrupt RNA−protein interactions in an NTP-dependent manner (*4*, *5*). For these reasons, DExH/D proteins have been primarily implicated in processes that involve the disassembly of RNA−RNA and RNA−protein interactions (*1*). However, exact physiological targets for most DExH/D proteins are not well-defined, and it is thus unclear whether all DExH/D proteins are exclusively disassembling RNA or RNA−protein complexes. In fact, it has recently been reported that some DEAD-box proteins, including human p68 and bacterial CrhR, promote the formation of RNA duplexes in vitro, in addition to RNA unwinding (*6*, *7*). These findings suggest that both unwinding and annealing activities, as well as a capacity to "tune" between RNA unwinding and duplex formation, may be important for the remodeling of RNA/RNP structure(s) by select DExH/D proteins. Yet, there is virtually no mechanistic understanding of whether and, if so, how these DEAD-box proteins coordinate RNA unwinding and annealing activities.

Here, we show in vitro that the DEAD-box protein DED1 from *Saccharomyces cerevisiae*, which is highly conserved among eukaryotes (*8*), has the ability to balance RNA unwinding with a profound strand annealing activity in a highly dynamic fashion. We demonstrate that DED1, in addition to its previously shown RNA helicase activity (*9*), also facilitates the formation of RNA duplexes. DED1 accelerates the bimolecular rate constant for RNA duplex formation to an extent that the diffusion limit for a bimolecular reaction is approached. We further show that DED1 establishes an ATP-dependent steady state between unwinding and strand annealing. The unwinding activity increases with the ATP concentration, whereas the annealing

[†] This work was supported by NIH Grant GM067700 to E.J.

* Corresponding author: Eckhard Jankowsky, Department of Biochemistry, School of Medicine, Case Western Reserve University, 10900 Euclid Ave., Cleveland, OH 44106. Tel, (216) 368-3336; fax, (216) 368-3419; e-mail, exj13@case.edu.

[1] Abbreviations: ATP, adenosine 5′-triphosphate; ADP, adenosine 5′-diphosphate; AMPPNP, adenosine 5′-(*β*,*γ*-imido)triphosphate; NTP, nucleoside 5′-triphosphate; RNP, ribonucleprotein; Tris, tris(hydroxylmethyl)aminomethane; DTT, dithiothreitol; EDTA, (ethylenedinitrilo)-tetraacetic acid; SDS, sodium dodecyl sulfate; PAGE, polyacrylamide gel electrophoresis; BSA, bovine serum albumin; bp, basepair; nt, nucleoside; wt, wild-type; NPH-II, nucleotide phosphohydrolase II; eIF4A, eukaryotic initiation factor 4A.

10.1021/bi0508946 CCC: $30.25
Published on Web 09/21/2005

activity decreases with the ATP concentration, and DED1 is thus able to modulate the balance between the two opposing activities. Moreover, the balance between duplex unwinding and formation strongly depends on the nature of the RNA substrate. Finally, we demonstrate that ADP influences the balance between unwinding and annealing even more than ATP at comparable concentrations and that the degree of this ADP-dependent modulation depends on the nature of the RNA substrate as well. These results expand the functional repertoire of DEAD-box proteins. Our observations reveal that DED1, by involving a significant strand annealing activity, is able to differentially regulate RNA remodeling for distinct substrates as a function of ATP and ADP concentration.

MATERIALS AND METHODS

Protein Expression and Purification. DED1 was expressed in *Escherichia coli* and purified as previously described (*5*). Homogeneity (>98%) and concentration of DED1 was assessed by SDS−PAGE and Coomassie staining. The $DED1_{\Delta C}$ mutant, in which 86 amino acid residues at the carboxyl terminus of DED1 were deleted, was generated by replacing the codon of T519 with a UAA stop codon using PCR-based mutagenesis. The PCR products were cloned into pET-22b and sequenced. The resulting plasmid was then transformed into BL21(DE3) (*9*). $DED1_{\Delta C}$ was expressed and purified as wtDED1. Homogeneity (>90%) and concentration of $DED1_{\Delta C}$ was assessed by SDS−PAGE and Coomassie staining. NPH-II was expressed in baculovirus-infected insect cells and purified as described (*10*). Purified eIF4A was a gift from Dr. W. Merrick (*11*).

RNA Substrate Preparation. RNA oligonucleotides were purchased from DHARMACON, and duplex substrates were prepared as described (*12*). Top strands of duplexes were labeled with [γ^{32}P]ATP, and RNA was quantified by scintillation counting. Substrates were formed as follows (duplex regions are underlined). S[16]: T16 + B41 (5′-AGCA CCGUAAAGACGC + 5′-GCGUCUUUACGG UGCU-UAAAACAAAACAAAACAAAACAAAA-3′). F[16]: T41 + B41 (5′-AAAACAAAACAAAACAAAACAAAAUAG-CACCGUAAAGACGC + 5′-GCGUCUUUACGGUGCU-UAAAACAAAACAAAACAAAACAAAA-3′). S[19]: T19 + B44 (5′-AGCACCGUAAAGACGCAGC-3′ + 5′-GCU-GCGUCUUUACGGUGCUUAAA ACA AAACAAAA-CAAAACAAAA).

Unwinding Reactions. Reaction mixtures (30 μL) containing 40 mM TrisHCl (pH 8.0), 50 mM NaCl, 0.5 mM $MgCl_2$, 2 mM DTT, 1 unit/μL RNasin, 0.01% NP40, and 0.5 nM ^{32}P-labeled RNA substrate were incubated with 600 nM DED1 for 5 min. DED1 at 600 nM was saturating with respect to the RNA substrates at all reaction conditions (data not shown). Reactions were performed in a temperature-controlled aluminum block at 19°C. All reactants were incubated at 19°C prior to the reaction to avoid temperature changes upon addition of components. Unwinding reactions were initiated by adding an equimolar mixture of $MgCl_2$ and ATP. For reactions including ADP and AMPPNP, ADP-$MgCl_2$ and AMPPNP-$MgCl_2$ were added together with ATP-$MgCl_2$ at the reaction start. At the times indicated, aliquots (3 μL) were removed and the reaction was stopped with a buffer containing 1% SDS, 50 mM EDTA, 0.1% xylene cyanol, 0.1% bromophenol blue, and 20% glycerol. Aliquots were applied to a 15% nondenaturing PAGE, and duplex and single-stranded RNA were separated at room temperature at 100 V/cm. Subsequently, gels were dried, and the radiolabeled RNAs were visualized and quantified with a Molecular Dynamics Phosphorimager and the ImageQuant 5.2 software (Molecular Dynamics).

Annealing Reactions. Reaction mixtures (30 μL) containing 40 mM TrisHCl (pH 8.0), 50 mM NaCl, 0.5 mM $MgCl_2$, 2 mM DTT, 1 unit/μL RNasin, and 0.01% NP40 were incubated with 600 nM DED1 and, where indicated, with MgATP, MgADP, or MgAMPPNP for 5 min. The duplex RNA substrates were denatured at 95 °C for 2 min to generate single-stranded RNAs. Reactions were performed in a temperature-controlled aluminum block at 19 °C. Annealing reactions were initiated by addition of 0.5 nM of the denatured substrate strands. Aliquots (3 μL) were removed at the times indicated, and reactions were stopped with the same buffer used to quench the unwinding reactions. Single-stranded and duplex RNAs were separated as described for the unwinding assays.

Data Analysis. The fractions of single-stranded and duplex RNA were determined from the relative amount of radiaoactivity in the respective bands (single strand, I^{ss}; duplex, I^{dpx}), measured with the ImageQuant 5.2 software (Molecular Dynamics). The fraction of single-stranded RNA was determined according to

$$\text{Frac ss} = I^{ss}(I^{ss} + I^{dpx})^{-1} \quad \text{(I)}$$

The fraction of duplex RNA was computed according to

$$\text{Frac dpx} = 1 - \text{Frac ss} \quad \text{(II)}$$

Observed rate constants $\boldsymbol{k}_{obs}^{(unw)}$ for unwinding reactions were determined by fitting time courses to the integrated rate law for a homogeneous first-order reaction:

$$\text{Frac ss} = A\{1 - \exp(-\boldsymbol{k}_{obs}^{(unw)} \cdot t)\} \quad \text{(III)}$$

A is the reaction amplitude. Bimolecular rate constants for strand annealing reactions, $\boldsymbol{k}_{obs}^{(ann)}$, were determined by fitting time courses to the integrated rate law for the bimolecular annealing reaction, considering that both strands were present at equal concentrations:

$$\text{Frac ss} = (1 + [\text{RNA}]_0 \cdot \boldsymbol{k}_{obs}^{(ann)} \cdot t)^{-1} \quad \text{(IV)}$$

$[RNA]_0$ is the concentration of each strand. Rate constants for unwinding ($\boldsymbol{k}_{unw}$) and annealing ($\boldsymbol{k}_{ann}$) at the ATP-dependent steady state between duplex formation and strand separation were determined based on the following kinetic scheme:

$$d[ss]/dt = \boldsymbol{k}_{unw}[dpx] - \boldsymbol{k}_{ann}[ss] \quad \text{(V)}$$

$$d[dpx]/dt = \boldsymbol{k}_{ann}[ss] - \boldsymbol{k}_{unw}[dpx] \quad \text{(VI)}$$

where dpx stands for duplex and ss stands for single strands. Solving the two differential equations, integrating, and rearranging for the fraction of single stranded RNA yields

$$\text{Frac ss} = \boldsymbol{k}_{unw}(\boldsymbol{k}_{unw} + \boldsymbol{k}_{ann})^{-1}(1 - \exp\{-(\boldsymbol{k}_{unw} + \boldsymbol{k}_{ann})t\}) \quad \text{(VII)}$$

Eq VII was used to fit the time courses of unwinding reactions at varying ATP, ADP, and AMPPNP concentrations. Note that the annealing rate constant here is treated as an apparent first-order rate constant, valid at the fixed concentration of DED1 (600 nM) and RNA (0.5 nM for each strand or the duplex). This mathematical treatment yields robust solutions by providing a simple analytical term for the integrated rate law, in contrast to a significantly more complex numerical solution that incorporates bimolecular rate constants for the annealing reactions. Controls showed that observed first-order rate constants ($\boldsymbol{k}_{\text{first}}^{\text{ann}}$) and observed second-order rate constants ($\boldsymbol{k}_{\text{second}}^{\text{ann}}$) for the same annealing reaction could be interconverted using an expression that equates first- and second-order half-lifes (concentration of both strands is equal) according to

$$\boldsymbol{k}_{\text{second}}^{\text{ann}} = \boldsymbol{k}_{\text{first}}^{\text{ann}}([\text{RNA}]_0 \ln 2)^{-1}$$

Discrepancies between the two rate constants as a result of this conversion were significantly smaller than the experimental error.

The dependencies of rate constants for unwinding and/or annealing or ratios of rate constants on ATP, ADP, or AMPPNP concentrations were analyzed by either fitting the respective curves to a hyperbolic binding isotherm

$$\boldsymbol{k}_x = \boldsymbol{k}_x^{\text{max}} \cdot [\text{NTP}] \cdot ([\text{NTP}] + \boldsymbol{K}_{\mathbf{m}})^{-1} \qquad \text{(VIII)}$$

or to a sigmoidal Hill binding isotherm

$$\boldsymbol{k}_x = \boldsymbol{k}_x^{\text{max}} \cdot [\text{NTP}]^{\boldsymbol{n}} \cdot ([\text{NTP}]^{\boldsymbol{n}} + \boldsymbol{K}_{\mathbf{m}}^{\boldsymbol{n}})^{-1} \qquad \text{(IX)}$$

where $\boldsymbol{k}_x$ is the value for the rate constant at a given ATP, ADP, or AMPPNP concentration; $\boldsymbol{k}_x^{\text{max}}$ is the rate constant (or ratio of rate constants) at ATP, ADP, or AMPPNP saturation; and $\boldsymbol{K}_{\mathbf{m}}$ represents the ATP, ADP, or AMPPNP concentration where the half-maximal effect is reached and $\boldsymbol{n}$ is the Hill coeffcient. Curve fitting was performed with Kaleidagraph (Synergy software).

RESULTS

DED1 Catalyzes Both Unwinding and Annealing of RNA Duplexes. To gain insight into the biochemical properties of DED1, we first tested the ability of the enzyme to unwind an RNA duplex substrate containing a 25 nucleotide overhang 3′ to a 16 basepair duplex region. DED1 readily separated the two strands in the presence of ATP (Figure 1A). Unwinding was only observed with ATP or dATP. Virtually no helicase activity was detected with other nucleoside triphosphates, and no significant strand separation occurred in the presence of the ATP analogue AMPPNP or in the presence of ADP (Figure 1B). These results show that the RNA helicase activity of DED1 is strictly dependent on adenosine triphosphates.

Unexpectedly, DED1 significantly accelerated the formation of an RNA duplex (Figure 1C,D). This annealing activity did not require ATP (Figure 1C). DED1 enhanced the bimolecular rate constant of spontaneous duplex formation of $(1.4 \pm 0.3) \times 10^6$ M^{-1} min^{-1} by more than 3 orders of magnitude to $(3.1 \pm 0.6) \times 10^9$ M^{-1} min^{-1} (Figure 2A). Significantly, the bimolecular rate constant for strand annealing in the presence of DED1 approaches the diffusion limit for a bimolecular reaction of $\sim 10^{10}$ M^{-1} min^{-1} (*13*).

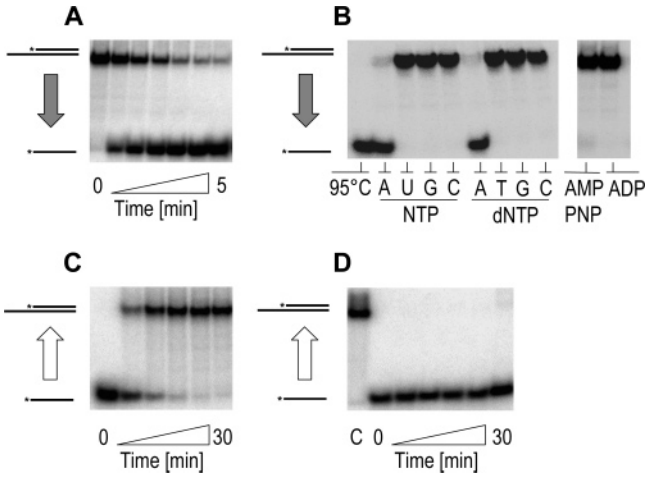

FIGURE 1: RNA unwinding and strand annealing activties of DED1. (A) Representative PAGE of an unwinding time course. Mobilities of duplex and single-stranded RNAs are indicated by the cartoons on the left. The block arrow emphasizes that the reaction was started with duplex RNA. The 0 time point represents the reaction before ATP addition. Aliquots were removed between 5 s and 5 min. (B) Unwinding reactions with various NTPs at 1 mM (left panel) and 1 mM AMPPNP and 1 mM ADP (right panel). Reactions were performed as described in Materials and Methods, except that ATP-$MgCl_2$ was replaced with equimolar mixtures of $MgCl_2$ and NTPs, dNTPs, AMPPNP, or ADP, as indicated underneath the gels. Reactions were incubated for 30 min. (C) Representative PAGE of a strand annealing time course with DED1. No ATP was present during the reaction. The block arrow indicates that the reaction was started with single-stranded RNA. The 0 time point represents the reaction before DED1 addition. Aliquots were removed from 0.5 to 30 min. (D) Representative PAGE of a strand annealing time course without DED1. Lane C indicates the control for the duplex.

To test whether this pronounced strand annealing activity was specific for DED1, we measured to which extent duplex formation was promoted by two other DExH/D enzymes, the DExH protein NPH-II and the DEAD-box protein eIF4A (Figure 2A). Both proteins increased the bimolecular annealing rate constant by approximately 1 order of magnitude over the basal rate constant. This increase is significant, yet 2 orders of magnitude less than the enhancement by DED1 (Figure 2A). These findings suggest that DExH/D proteins do not generally facilitate duplex formation to the level seen with DED1.

Nonetheless, a capacity to promote both duplex unwinding and strand annealing in vitro had been previously reported for three other DEAD-box proteins (human p68 and p72, and CrhC from cyanobacteria), although it is unknown whether those proteins enhance the annealing rate constant to the level measured for DED1 (*6*, *7*). However, we noted that these proteins share with DED1 a characteristic C-terminus containing clusters of arginines and glycines, in addition to the commonly conserved regions of DEAD-box proteins (Figure 2B). To ascertain the importance of the C-terminus for the annealing activity of DED1, we deleted the C-terminal 86 amino acids from DED1, expressed and purified the mutant protein $DED1_{\Delta C}$, and measured the annealing activity of this altered peptide (Figure 2A). With saturating $DED1_{\Delta C}$, the bimolecular rate constant of duplex formation was decreased approximately 12-fold, compared to wild-type DED1 (Figure 2A). The unwinding activity was

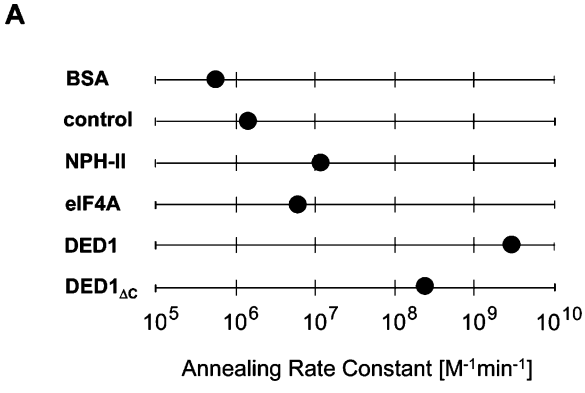

B

```
                Motif VI
p68   YPNSSEDYIHRIGRTARSTKTGTAYTFFTPNNIKQVSDLISVLREANQAINPKLLQLVED  477
p72   YPNSSEDYVHRIGRTARSTNKGTAYTFFTPGNLKQARELIKVLEEANQAINPKLMQLVDH  475
DED1  LPSDVDDYVHRIGRTGRAGNTGLATAFFNSENSNIVKGLHEILTEANQEVPSFLKDAMMS  535
CrhR  LPDNAETYIHRIGRTGRAGKTGKAIALVEPIDRRLLRSIENRL-KQQIEVCTIPNRSQVE  380

p68   R-----GSGRSRGRGG--------MKDDRRDRYSAGKRGG----FNTFRDRENYDRG-YS  519
p72   RGGGGGGGGRSRYRTTSSANNPNLMYQDECDRRLRGVKDGGRRDSASYRDRSETDRAGYA  535
DED1  AP-----GSRSNSRRGGFGRNNNRDYRKAGGASAGGWGSSRSRDNSFRGGSGWG------  589
CrhR  [381-448]KPVLRRGRNAGGGQNKSGGGYQGKPGKPRRSSGGRRPAYSDRQQ-------  492
```

FIGURE 2: Pronounced strand annealing activity is specific for DED1. (A) Observed rate constants for strand annealing reactions in the presence of different proteins. Points on the scaled bars (note log scale) indicate the observed annealing rate constants (k_{obs}^{ann}), which were calculated by fitting time courses of annealing reactions to eq IV (Materials and Methods). Time courses for each protein given on the left were constructed from at least 6 time points. Each time point was determined in at least three independent experiments. All reactions were performed at identical salt and buffer conditions with identical RNA concentrations (Materials and Methods). Proteins were present in the reaction in the following concentrations: BSA, 1 μM; control, no protein added; NPH-II, 50 nM (saturating with respect to the RNA (*10*); eIF4A, 1 μM (maximal possible concentration (*11*); DED1, 600 nM (saturating with respect to the RNA); $DED1_{\Delta C}$, 600 nM (saturating with respect to the RNA). $DED1_{\Delta C}$ lacked the C-terminal 86 amino acids (Materials and Methods). (B) Sequence alignment of the C-termini of DEAD-box proteins with annealing activity in vitro. Alignments were generated with CLUSTAL X (*32*). Numbers indicate amino acids counted from the N-terminus.

only reduced by a factor of ~1.2 (Figure 3F). This result shows that the C-terminus with the characteristic RG-clusters contributes to the annealing activity of DED1, yet the ability to promote duplex formation does not reside exclusively within this part of DED1.

DED1 Establishes an ATP-Dependent Steady State between RNA Unwinding and Strand Annealing. Having established the ability of DED1 to profoundly facilitate RNA duplex formation without ATP, we next investigated whether DED1 also promoted strand annealing in the presence of ATP. With 0.1 mM ATP, DED1 readily catalyzed duplex formation (Figure 3A). However, the reaction did not proceed to completion, as observed without ATP (cf. Figure 1C). Instead, a distinct reaction amplitude was reached (Figure 3A,C). This reaction amplitude was not caused by inactivation of the enzyme or ATP depletion during the reaction, as DED1 remained fully active with respect to both unwinding and annealing for more than 60 min under all reaction conditions (data not shown). Unwinding time courses at 0.1 mM ATP also showed a clear reaction amplitude that was virtually identical to the amplitude of the annealing reaction at the same ATP concentration (Figure 3B,C). At 0.25 mM ATP, reaction amplitudes for the unwinding and annealing

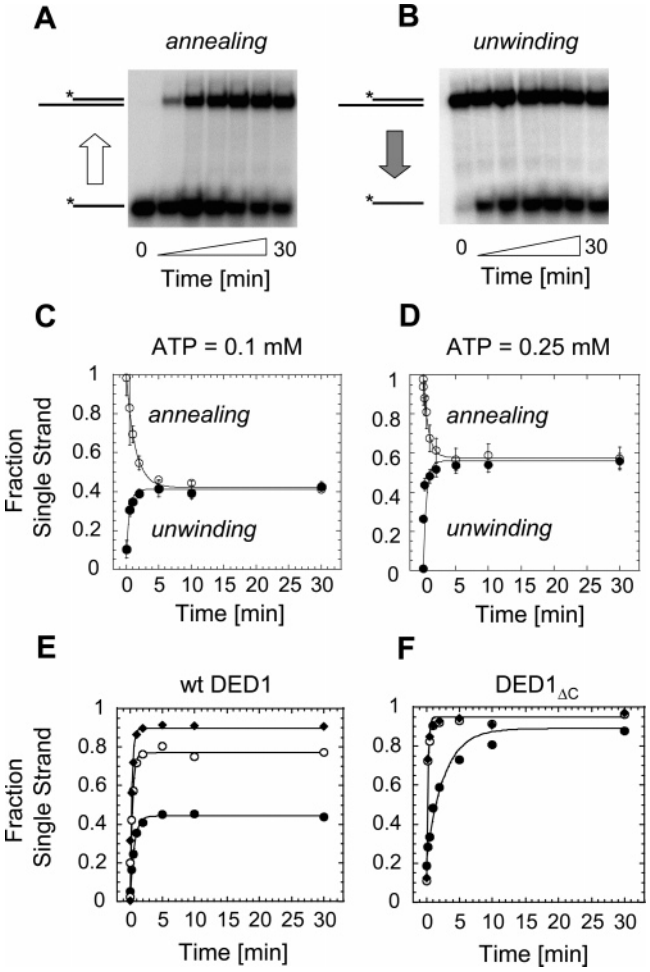

FIGURE 3: DED1-catalyzed ATP-dependent steady state between RNA unwinding and strand annealing. (A) Representative PAGE for a strand annealing reaction in the presence of DED1 and 0.1 mM ATP. The RNAs were identical to those used in Figure 1. The arrow indicates that the reaction was started with single-stranded RNA. Aliquots were removed from the reaction at the times indicated in panel C. (B) Representative PAGE for an unwinding reaction in the presence of DED1 and 0.1 mM ATP. The arrow indicates that the reaction was started with duplex RNA. Aliquots were removed at the times indicated in panel D. (C) Time courses of strand annealing (○) and unwinding (●) reactions in the presence of DED1 and 0.1 mM ATP. Data points represent the average of at least three independent reactions; error bars indicate one standard deviation. The line through the data points represents the best fit to the integrated form of a homogeneous first-order rate law (eq III, Materials and Methods). The reaction amplitude $A^{unw} = 0.41 \pm 0.02$. The line through the annealing time course represents the best fit to the integrated form of a homogeneous first-order rate law (eq IV, Materials and Methods). $A^{ann} = 0.43 \pm 0.02$. (D) Time courses of strand annealing (○) and unwinding (●) reactions in the presence of DED1 and 0.25 mM ATP. Data were measured, and rate constants and reaction amplitudes were determined as in panel C. $A^{unw} = 0.56 \pm 0.05$; $A^{ann} = 0.54 \pm 0.02$. (E) Time courses for unwinding reactions with wtDED1 at 0.1 mM ATP (●), 0.5 mM ATP (○), and 2 mM ATP (◆). Time courses were fit to eq III, yielding the following values: at 0.1 mM ATP, $k_{obs}^{unw} = 1.5 \pm 0.1$ min^{-1}, $A^{unw} = 0.42 \pm 0.02$; at 0.5 mM ATP, $k_{obs}^{unw} = 3.0 \pm 0.2$ min^{-1}, $A^{unw} = 0.73 \pm 0.02$; and at 2 mM ATP, $k_{obs}^{unw} = 3.7 \pm 0.4$ min^{-1}, $A^{unw} = 0.90 \pm 0.05$. (F) Time courses for $DED1_{\Delta C}$-catalyzed unwinding reactions at 0.1 mM ATP (●), 0.5 mM ATP (○), and 2 mM ATP (◆). Time courses were fit to eq III, yielding the following values: at 0.1 mM ATP, $k_{obs}^{unw} = 0.6 \pm 0.2$ min^{-1}, $A^{unw} = 0.90 \pm 0.02$; at 0.5 mM ATP, $k_{obs}^{unw} = 2.5 \pm 0.3$ min^{-1}, $A^{unw} = 0.97 \pm 0.03$; and at 2 mM ATP, $k_{obs}^{unw} = 2.8 \pm 0.3$ min^{-1}, $A^{unw} = 0.97 \pm 0.03$.

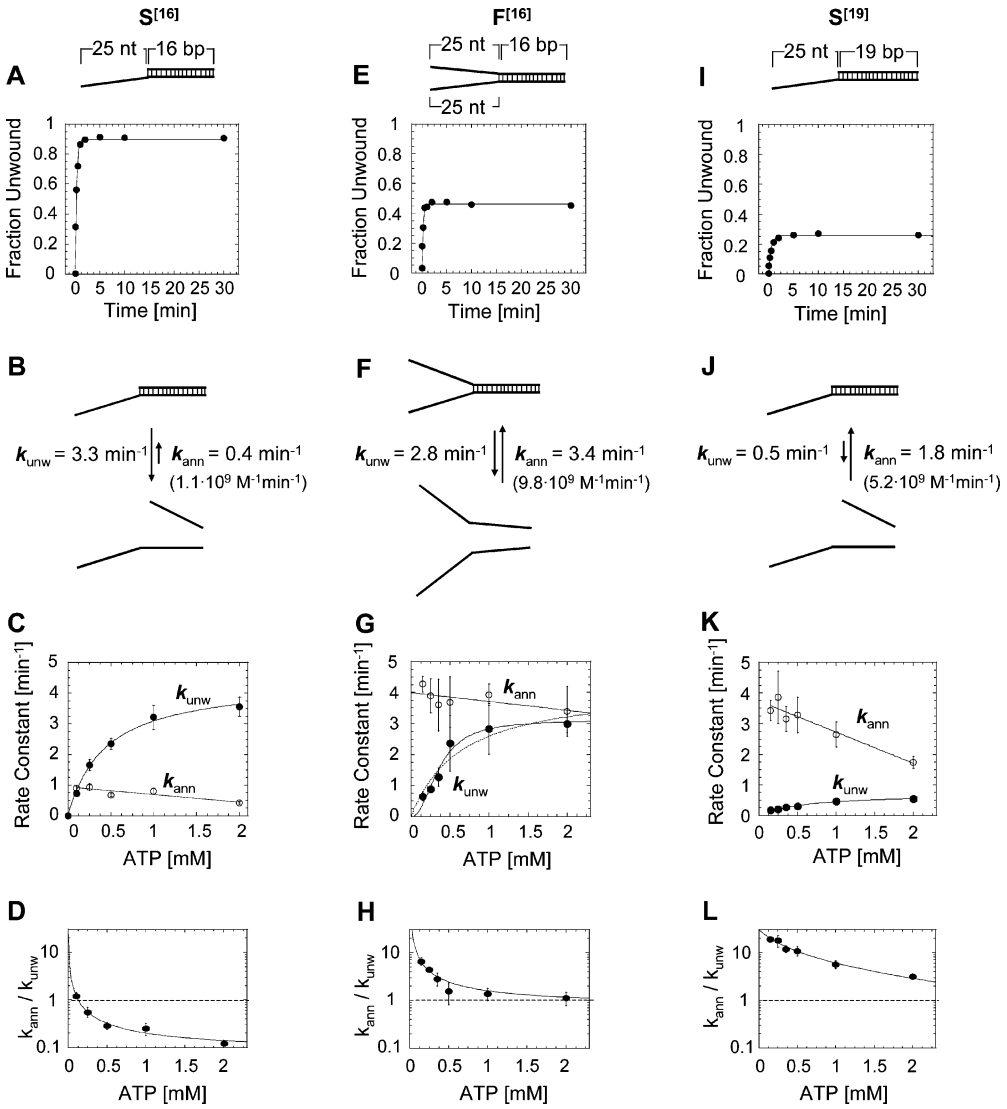

FIGURE 4: Dependence of unwinding and annealing rate constants on ATP-concentration and the nature of the RNA substrate. (A) Representative unwinding time course for $S^{[16]}$ with 2 mM ATP. Reaction amplitude $A^{unw} = 0.90 \pm 0.05$. (B) Rate constants for both unwinding and annealing reactions with $S^{[16]}$ at 2 mM ATP. The time course in panel A was fit to eq VII (Materials and Methods), yielding the indicated rate constants. For the annealing reaction, both apparent first-order rate constants and bi-molecular rate constants are given; for interconversion, see Materials and Methods. (C) Dependence of unwinding (●) and annealing (○) rate constants on ATP concentration. Rate constants were determined as described in panel B from unwinding time courses at each ATP concentration. Data points are the average value from multiple independent measurements; error bars indicate one standard deviation. The curve for unwinding rate constants vs [ATP] was fitted to a binding isotherm (eq VIII, Materials and Methods), yielding $\boldsymbol{k}_{unw}^{[max]} = 4.4 \pm 0.2$ min^{-1} and $\boldsymbol{K}_{\mathbf{m}}^{unw} = 0.43 \pm 0.04$ mM. The line through the annealing rate constants vs [ATP] represents a linear trend. (D) Ratio of unwinding and annealing rate constants vs [ATP]. The ratio was calculated from the values given in panel C. Note the logarithmic scale of the *y*-axis. The dashed line emphasizes the ratio of 1; values above the line indicate predominant annealing, values below the line predominant unwinding activity. The solid line represents a hyperbolical trend. (E) Representative unwinding timecourse for $F^{[16]}$ with 2 mM ATP ($A = 0.45 \pm 0.05$). (F) Rate constants for both unwinding and annealing reactions with $F^{[16]}$ at 2 mM ATP. (G) Dependence of unwinding (●) and annealing rate (○) constants on ATP concentration for $F^{[16]}$. Rate constants were determined as in panel C. The curve for unwinding rate constants vs [ATP] was fit to a sigmoidal binding isotherme (eq IX), yielding $\boldsymbol{k}_{unw}^{[max]} = 3.1 \pm 0.3$ min^{-1}, $\boldsymbol{K}_{\mathbf{m}}^{unw} = 0.36 \pm 0.05$ mM, and a Hill coefficient of $\boldsymbol{n} = 2.2 \pm 0.6$. The dashed line illustrates a hyperbolic binding isotherm (eq VIII). The line through the annealing rate constants vs [ATP] represents a linear trend. (H) Ratio of unwinding and annealing rate constants vs [ATP] for $F^{[16]}$. The solid line represents a hyperbolic trend. (I) Representative unwinding timecourse for $S^{[19]}$ with 2 mM ATP ($A = 0.24 \pm 0.02$). (J) Rate constants for both unwinding and annealing reactions with $S^{[19]}$ at 2 mM ATP. (K) Dependence of unwinding (●) and annealing (○) rate constants on ATP concentration for $S^{[19]}$. Rate constants were determined as in panel C. Unwinding rate constants vs [ATP] were fit to a hyperbolic binding isotherm (eq VIII), yielding $\boldsymbol{k}_{unw}^{[max]} = 0.69 \pm 0.04$ min^{-1} and $\boldsymbol{K}_{\mathbf{m}}^{unw} = 0.55 \pm 0.08$ mM. (L) Ratio of unwinding and annealing rate constants vs [ATP] for $S^{[19]}$. The solid line indicates a hyperbolic trend.

process were virtually identical too (Figure 3D). Notably, a larger fraction of single-stranded RNA was formed at 0.25 mM ATP than at 0.1 mM ATP (Figure 3D).

These observations show that DED1 generated the same fraction of duplex and single-stranded RNAs at a given ATP concentration, regardless of whether the reaction was initiated from single strands or from the duplex. Thus, observed amplitudes are not the result of a stable dead-end complex between DED1 and one (or both) of the RNA strands. In this case, unwinding would have proceeded to completion, as the dead-end complex would have "pulled" all RNA toward the single-stranded products. Instead, the data were

consistent with DED1 simultaneously exhibiting two mechanistically distinct activities, ATP-independent annealing and ATP-dependent unwinding. As a result, a steady state between duplex and single-stranded RNA is reached. Since the poise of a steady state between two opposing processes is determined by the ratio of the two reaction rate constants, a greater fraction of single-stranded RNA at a higher ATP concentration suggested that increasing ATP concentrations enhanced the rate constant for the unwinding process, relative to that for the annealing reaction. This notion was further supported by time courses for unwinding reactions over a larger range of ATP concentrations (Figure 3E). Reaction amplitudes (fraction of single-stranded RNA) increased with the ATP concentrations, indicating that higher ATP concentrations enhanced the rate constant of unwinding, relative to the rate constant for annealing.

To establish further the ability of DED1 to promote an ATP-dependent steady state between unwinding and annealing, we directly tested a central prediction: reaction amplitudes at a given ATP concentration result from a distinct ratio of unwinding and annealing rate constants. We reasoned that measuring the ATP dependence of the reaction amplitudes with a variant of DED1 that promoted both processes with a different velocity ratio should yield different amplitudes, compared to reactions with wtDED1 under identical reaction conditions. Therefore, unwinding reactions with the C-terminal DED1 deletion mutant ($DED1_{\Delta C}$), which favors unwinding over annealing, compared to wtDED1 (Figures 2A and 3F), should yield greater amplitudes than wtDED1. This expectation was confirmed. Reaction amplitudes for $DED1_{\Delta C}$ were significantly higher than with wtDED1 under identical conditions (Figure 3E,F). This result clearly corroborates the notion that DED1 establishes an ATP-dependent steady state between unwinding and annealing reactions.

ATP Modulates the Balance between RNA Unwinding and Strand Annealing. To understand the mechanism by which DED1 balanced catalysis of the two opposing processes, it was of interest to assess quantitatively the effect of the ATP concentration on the ratio between unwinding and annealing rate constants. To this end, we determined unwinding and annealing rate constants at different ATP concentrations (Figure 4). We note that each individual rate constant is likely to describe a complex reaction consisting of multiple steps.

The unwinding rate constant increased by a factor of 4.9 between 0.1 and 2 mM ATP (Figure 4C). The annealing rate constant decreased by a factor of 2.1 between 0.1 and 2 mM ATP (Figure 4C). This decrease, although smaller than the increase in the unwinding rate constant, is significant. We confirmed independently the ATP-mediated inhibition of the annealing activity in separate annealing reactions, and we also verified that the measured changes in both unwinding and annealing rate constants were not caused by an increase in free Mg^{2+} ions, which accompany the ATP (data not shown).

Thus, our data show that ATP exerts differential effects on unwinding and annealing rate constants. As a consequence, DED1 is able to modulate between unwinding and annealing activities in an ATP-dependent fashion. At low ATP concentrations (ATP < 0.1 mM), annealing is favored over unwinding; at high ATP (ATP > 0.1 mM), the reverse is true (Figure 4D). This observation suggests that the ATP concentration is critical not only for establishing the steady state between unwinding and annealing but also for determining the ratio between the rate constants for both processes.

The Balance between Unwinding and Annealing Activities of DED1 Depends on the RNA Substrate. We next tested whether the nature of the RNA substrate affected the activities of DED1. We generated a forked RNA complex containing unpaired nucleotides 5′ and 3′ to the duplex region of the substrate used above ($F^{[16]}$, Figure 4E). Although the forked RNA complex differed only in unstructured regions from the RNA used above ($S^{[16]}$), time courses at 2 mM ATP showed a significantly lower reaction amplitude (Figure 4E). (Note that in all reactions (i) DED1 was present at saturating concentrations with respect to the substrates, (ii) the concentration of all substrates was held constant at 0.5 nM, and (iii) the basal rates for spontaneous annealing were within the same order of magnitude for all substrates.) Interestingly, the unwinding rate constant for $F^{[16]}$ was only slightly lower than for $S^{[16]}$, whereas the annealing rate constant was significantly greater for $F^{[16]}$ (Figure 4F). These findings suggest that the presence of unpaired substrate regions impacts the annealing activity of DED1 while affecting the unwinding activity only slightly.

We then determined unwinding and annealing rate constants for $F^{[16]}$ over a range of ATP concentrations (Figure 4G). The unwinding rate constant increased by a factor of 4.3 between 0.1 mM and 2 mM ATP (Figure 4G). This increase is similar to the extent by which the unwinding rate constant increased with the ATP concentration for $S^{[16]}$ (cf. Figure 4C). The dependence of the unwinding rate constants on the ATP concentration for $F^{[16]}$ was better described by a sigmoidal curve, rather than by a hyperbola as for $S^{[16]}$. DED1 may thus interact differently with each of the substrates and perhaps function as an oligomer on $F^{[16]}$ (Figure 4G). The annealing rate constant for $F^{[16]}$ decreased by a factor of 1.2 between 0.1 and 2 mM ATP (Figure 4G). This decrease does not exceed the error range of the experiment and/or the effect caused by the Mg^{2+} that accompanies the ATP (data not shown). Thus, in contrast to the observations made with $S^{[16]}$, no clear effect of ATP on the annealing rate constant could be detected for $F^{[16]}$, indicating that the unpaired RNA region in the top strand of the substrate affected not only the overall annealing rate constant but also the degree by which this annealing rate constant was influenced by the ATP concentration.

Despite the less pronounced ATP effect on the annealing activity of DED1 with $F^{[16]}$, the ratio between annealing and unwinding rate constants decreased with the ATP concentration (Figure 4H). Notably, at all ATP concentrations tested with the given substrate concentrations, the annealing rate constant outweighed the unwinding rate constant; that is, DED1 was a much stronger "annealer" for $F^{[16]}$ than for $S^{[16]}$, even though the annealing activity was attenuated at higher ATP concentrations (Figure 4H). The results with $F^{[16]}$, taken together with the data obtained with $S^{[16]}$, thus indicate that unpaired substrate regions affect the ATP-dependent modulation between RNA unwinding and strand annealing.

We next tested how the length of the duplex region influenced the activities of DED1. To this end, we generated a substrate where we extended the duplex region of the complex with the single overhang ($S^{[19]}$, Figure 4I). Unwinding time courses at 2 mM ATP showed a smaller amplitude

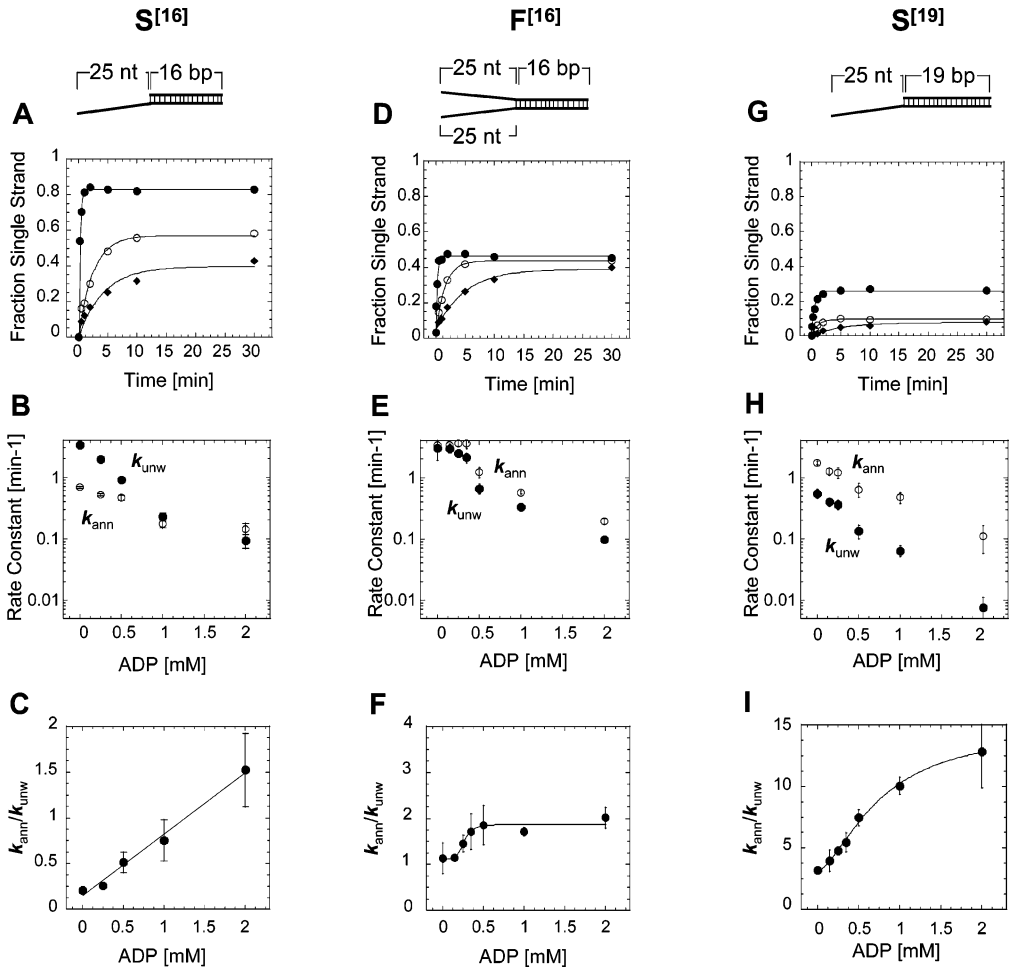

FIGURE 5: ADP-dependent modulation of unwinding and annealing activities of DED1. (A) Representative unwinding timecourses for $S^{[16]}$ in the presence of 2 mM ATP without ADP (●, reaction amplitude $A = 0.83 \pm 0.07$), 1 mM ADP (○, $A = 0.57 \pm 0.02$), and 2 mM ADP (♦, $A = 0.39 \pm 0.03$). (B) Dependence of unwinding (●) and annealing (○) rate constants for $S^{[16]}$ on ADP concentration. Rate constants were determined as described in Figure 4B. (C) Ratio of unwinding and annealing rate constants vs [ADP] for $S^{[16]}$. Values were calculated as in Figure 4D. The line represents a linear trend. (D) Representative unwinding timecourses for $F^{[16]}$ in the presence of 2 mM ATP without ADP (●, $A = 0.45 \pm 0.05$), 1 mM ADP (○, $A = 0.40 \pm 0.01$), and 2 mM ADP (◆, $A = 0.34 \pm 0.01$). (E) Dependence of unwinding (●) and annealing (○) rate constants for $F^{[16]}$ on ADP concentration. Rate constants were determined as described in Figure 4B. (F) Ratio of unwinding and annealing rate constants vs [ADP] for $F^{[16]}$. Values were calculated as in Figure 4D. The solid line indicates a sigmoidal trend. (G) Representative unwinding timecourses for $S^{[19]}$ in the presence of 2 mM ATP without ADP (●, $A = 0.24 \pm 0.02$), 1 mM ADP (○, $A = 0.10 \pm 0.01$), and 2 mM ADP (◆, $A = 0.07 \pm 0.01$). (H) Dependence of unwinding (●) and annealing (○) rate constants for $S^{[19]}$ on ADP concentration. Rate constants were determined as described in Figure 4B. (I) Ratio of unwinding and annealing rate constants vs [ADP] for $F^{[16]}$. Values were calculated as in Figure 4D. The line represents a sigmoidal trend.

than identical reactions with $F^{[16]}$ and $S^{[16]}$ (Figure 4I). The unwinding rate constant was considerably lower than for the two other substrates, whereas the annealing rate constant was greater than for $S^{[16]}$, yet smaller than for $F^{[16]}$ (Figure 4J). The unwinding rate constant increased, while the annealing rate constant decreased with increasing ATP concentrations (Figure 4K). The relative changes in the rate constants were similar to those observed for $S^{[16]}$ (cf. Figure 4C). Notably, DED1 catalyzed predominantly annealing with $S^{[19]}$ over the entire range of ATP concentrations. Increasing ATP concentrations attenuated the annealing activity of DED1 (Figure 4L).

Collectively, the data with the three different substrates demonstrate that the nature of the substrate influences (i) the balance by which DED1 catalyzes disruption and formation of RNA duplexes and (ii) the degree by which ATP modulates the ratio between unwinding and annealing.

ADP Also Modulates the Balance between RNA Unwinding and Strand Annealing. Having demonstrated an ATP-dependent modulation of the balance between unwinding and annealing activities of DED1, we wondered whether the other prevalent cellular nucleoside phosphate, ADP, also affected the activities of DED1. ADP itself did not promote substrate unwinding, as shown above (Figure 1B). To ascertain the effect of ADP on both unwinding and annealing rate constants, we conducted unwinding reactions with the three substrates tested above in the presence of 2 mM ATP and increasing amounts of ADP (Figure 5). The ATP concentration of 2 mM was chosen in order to obtain significant reaction amplitudes for all substrates (Figure 4).

Amplitudes of unwinding reactions with $S^{[16]}$ decreased with increasing ADP concentrations (Figure 5A), immediately indicating that annealing was favored over unwinding at higher ADP concentrations. Unwinding rate constants declined by a factor of 36.6 between 0 and 2 mM ADP (Figure 5B). Annealing rate constants also declined between 0 and 2 mM ADP, but only by a factor of 4 (Figure 5B). Thus, the relative decline of both rate constants differed, and

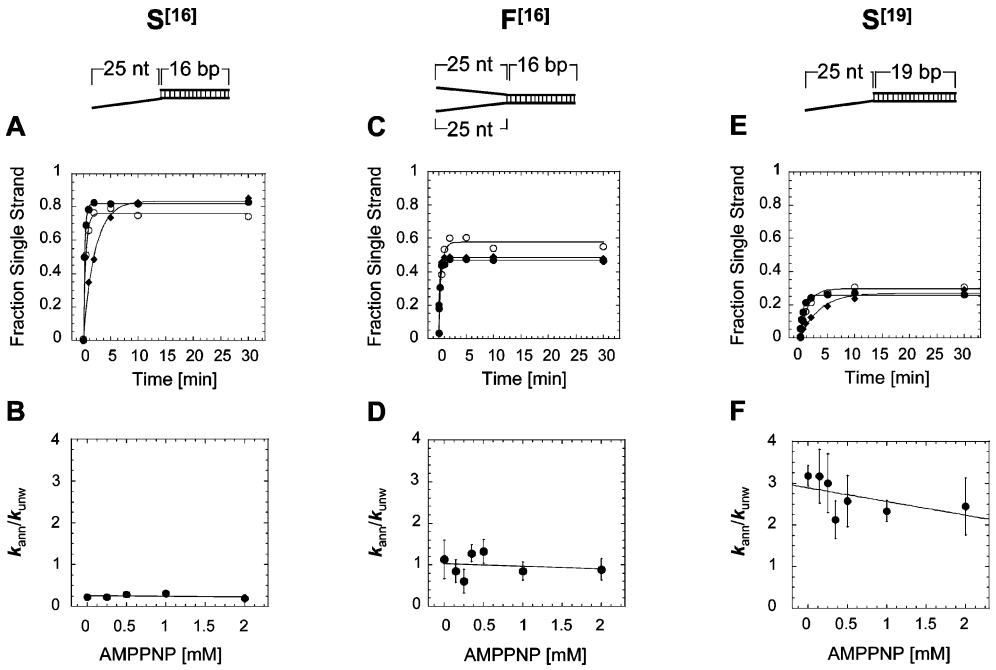

FIGURE 6: Effects of AMPPNP on unwinding and annealing activities of DED1. (A) Representative unwinding timecourses for $S^{[16]}$ in the presence of 2 mM ATP without AMPPNP (●, $A = 0.82 \pm 0.08$), 1 mM AMPPNP (○, $A = 0.76 \pm 0.06$), and 2 mM AMPPNP (◆, $A = 0.84 \pm 0.08$). (B) Ratio of unwinding and annealing rate constants vs [AMPPNP] for $S^{[16]}$. Values were calculated as in Figure 4D. The line represents a linear trend. (C) Representative unwinding timecourses for $F^{[16]}$ in the presence of 2 mM ATP without AMPPNP (●, $A = 0.45 \pm 0.05$), 1 mM AMPPNP (○, $A = 0.55 \pm 0.10$), and 2 mM AMPPNP (◆, $A = 0.47 \pm 0.06$). (D) Ratio of unwinding and annealing rate constants vs [AMPPNP] for $F^{[16]}$. Values were calculated as in Figure 4D. The line represents a linear trend. (E) Representative unwinding timecourses for $S^{[19]}$ in the presence of 2 mM ATP without AMPPNP (●, $A = 0.24 \pm 0.02$), 1 mM AMPPNP (○, $A = 0.29 \pm 0.03$), and 2 mM AMPPNP (◆, $A = 0.27 \pm 0.01$). (F) Ratio of unwinding and annealing rate constants vs [AMPPNP] for $S^{[19]}$. Values were calculated as in Figure 4D. The line represents a linear trend.

as a result, annealing was favored over unwinding at higher ADP concentrations (Figure 5C).

The nonhydrolyzable ATP analogue AMPPNP did not alter the balance between the two activities in a comparable fashion, even though increasing concentrations of AMPPNP inhibited both unwinding and annealing activities (Figure 6A,B). Moreover, increasing concentrations of free Mg^{2+} did not change the ratio between unwinding and annealing rate constants (data not shown). Thus, the ADP-dependent alteration of the balance between unwinding and annealing was not due to general inhibition of DED1.

Taken together, the above data provide the following insights. First, the balance between unwinding and annealing can be modulated by ADP. Second, ADP modulates the balance between unwinding and annealing activities to a higher degree than comparable ATP concentrations. Third, the ADP-mediated modulation is accomplished through a differential inhibition of unwinding and annealing activities.

The Degree of the ADP-Dependent Modulation between Unwinding and Annealing Depends on the RNA Substrate. The observed ADP-dependent alteration of the DED1 activity with $S^{[16]}$ raised the question whether the degree of this ADP-dependent modulation would also differ for distinct substrates. We therefore measured unwinding timecourses with increasing ADP concentrations with the substrates $F^{[16]}$ and $S^{[19]}$ (Figure 5D,G).

With $F^{[16]}$, reaction amplitudes decreased only slightly with increasing ADP (Figure 5D). This observation indicates a smaller degree of modulation between unwinding and annealing than seen with $S^{[16]}$ (cf. Figure 5A). Nonetheless, both unwinding and annealing rate constants declined with increasing ADP concentrations (Figure 5E). While the unwinding rate constant decreased by a factor of 28 between 0 and 2 mM ADP, the annealing rate constant decreased by a factor of 17 between 0 and 2 mM ADP (Figure 5E). Thus, the unwinding rate constant was affected to a degree similar to that seen with $S^{[16]}$. The annealing rate constant was significantly more decreased by ADP with $F^{[16]}$. Consequently, the ratio between both rate constants did not change as dramatically as with $S^{[16]}$ (Figure 5F). These observations show that the degree by which ADP modulates the balance between unwinding and annealing depends on the nature of the substrate too and that the presence of an additional unpaired region in the RNA substrate has a notable effect.

With $S^{[19]}$, amplitudes of unwinding timecourses also declined with increasing ADP concentrations (Figure 5G). The unwinding rate constant decreased by a factor of 18 between 0 and 2 mM ADP; the annealing rate constant decreased by a factor of 4.2 between 0 and 2 mM ADP (Figure 5H). Thus, ADP inhibited unwinding of a 19 bp duplex slightly (yet significantly) less than unwinding of the 16 bp duplexes in $S^{[16]}$ and $F^{[16]}$ (Figure 5B,E). ADP-mediated inhibition of the annealing rate constant for $S^{[19]}$, however, was similar to the inhibition observed for $S^{[16]}$ and significantly smaller than the inhibition seen for $F^{[16]}$ (Figure 5E). Notwithstanding, the ratio of unwinding and annealing rate constants changed for $S^{[19]}$ with increasing ADP concentrations such that annealing was increasingly favored over unwinding at higher ADP concentrations (Figure 5I).

AMPPNP did not alter the ratio between unwinding and annealing rate constants for either $F^{[16]}$ or $S^{[19]}$ substrate to the extent of the effects observed with ADP (Figure 6C−

F). These observations further demonstrate that the balance between unwinding and annealing activities is altered by ADP and not by general inhibition of DED1 with ATP analogues such as AMPPNP.

DISCUSSION

We have shown here that the DEAD-box protein DED1 strongly promotes RNA strand annealing, in addition to its ability to unwind RNA duplexes. We have further demonstrated that the balance between these two opposing activities is modulated by ATP and ADP concentrations and also depends on the nature of the RNA substrate. These features enable DED1 to regulate RNA remodeling in response to ATP and ADP concentrations and to features of the RNA substrate.

The strand annealing activity of DED1 is profound. Under our reaction conditions, DED1 enhances the rate constant for duplex formation by more than 3 orders of magnitude, up to a level that approaches the diffusion limit for a bimolecular reaction (*13*). This large increase of the annealing rate constant significantly exceeds enhancements reported for most other proteins that promote duplex formation, such as Ncp7, p53, or gBP21 (*14*−*16*).

Two other RNA helicases tested here did not display annealing activity comparable to that of DED1, although these enzymes did enhance the annealing rate constant by approximately 1 order of magnitude, which is significant. These observations suggest that RNA helicases may commonly promote strand annealing by an order of magnitude above the basal rate constant, perhaps by neutralizing charges through binding to the RNA backbone (*17*).

To our knowledge, only the RNA binding protein hnRNP A1 has been shown to accelerate strand annealing to the level seen with DED1 (*18*). Interestingly, hnRNP A1 contains, in addition to its RRM domains, a C-terminus rich in glycines and arginines. Removal of this C-terminus decreases the annealing activity of hnRNP A1 by an order of magnitude (*18*). DED1 also contains an RG-rich C-terminus, and as shown here, the removal of this C-terminus decreases the annealing activity of DED1 by an order of magnitude, too. Moreover, three other DEAD-box helicases containing such RG-rich C-termini (human p68 and p72 and cyanobacterial CrhR, Figure 2) have recently been shown to promote strand annealing as well (*6*, *7*), although it is unknown whether these proteins enhance the annealing rate constant to the level seen with DED1. Collectively, these findings make it attractive to hypothesize that C- or N-terminal RG-clusters may confer a pronounced ability to promote strand annealing to a diverse range of proteins. The exact role of RG-rich termini in RNA strand annealing is presently unknown, but it may be possible that the arginines neutralize charges of the sugar phosphate backbones of the RNA strands (*19*). Such charge neutralization is known to facilitate strand annealing (*18*). Glycines may provide the peptide (segment) with the flexibility necessary to adapt to different RNA structures or to allow for induced fit between RNA and protein (*20*).

Despite the prominence of the C-terminal RG-clusters, the strand annealing activity of DED1 most likely involves the helicase core domain with the ATP-binding site as well, enabling the enzyme to affect duplex formation with ADP and ATP. An influence of ATP on the annealing activity has also been observed for the cyanobacterial DEAD-box protein CrhR (*6*). However, in contrast to DED1, CrhR promotes duplex formation only in the presence of ATP.

A central insight of the present work is the capacity of DED1, and possibly other similar DEAD-box proteins, to establish a steady state between duplex disruption and formation. Significantly, duplex unwinding and strand annealing by DED1 are not microscopic reversals of the same reaction, but two distinct processes, each of which utilizes nucleotide cofactors differently. RNA unwinding is strictly dependent on the hydrolysis of ATP, whereas strand annealing does not require ATP hydrolysis or, inversely, ADP and P_i to form ATP. Nonetheless, both ATP and ADP affect the annealing reaction too, and it is also likely that both unwinding and annealing activities employ overlapping or even identical regions in DED1. That is, the two activities are unlikely to reside in completely different parts of the enzyme.

The employment of two distinct activities for unwinding and strand annealing constitutes a critical mechanistic distinction between DED1 and proteins with RNA or DNA chaperone activity, which also promote both disruption and formation of RNA duplexes (reviewed in ref *21*). These "traditional" RNA/DNA chaperones do not utilize NTPs or other cofactors and are only able to balance unwinding and annealing through protein binding, that is, through the microscopic reversal of helix destabilization and facilitation of annealing (*21*). In contrast, DED1 can utilize ATP and ADP to significantly affect the balance between RNA unwinding and strand annealing. The ATP-dependent scaling of the balance between unwinding and annealing is the sum of opposite effects of ATP on each of the activities. ADP, on the other hand, inhibits both unwinding and annealing, presumably by interfering with ATP binding. However, ADP inhibits both unwinding and annealing to a different degree, and as a result, an increase in ADP concentration favors the annealing activity.

The exact mechanisms by which ADP and ATP impact strand annealing are not yet clear. However, our data suggest that DED1, when bound to the RNA in the presence of ATP or ADP, adopts conformations less favorable for the facilitation of strand annealing, compared to DED1 without cofactors. This conclusion can be drawn because DED1 was present at saturating concentrations with respect to the RNA, even at the highest ADP and ATP concentration used.

In addition to the ATP- and ADP-dependence of the steady state between unwinding and annealing, we also found a sensitivity of DED1 to the nature of the RNA substrate. The unwinding rate constant decreases with the extent of the duplex region, but is largely insensitive to the overall length of the RNA. This observation is consistent with the proposed limited processivity of DED1 (*5*). The annealing rate constant increased with the overall length of the RNA, regardless of whether the RNA was structured or not (Figure 4). In addition, the increased length of RNA made the annealing rate constant more susceptible to ADP modulation (Figure 5). As a result, additional unpaired substrate regions impact the balance between unwinding and annealing activities as well as the degree by which this balance is modulated by ATP and ADP. Therefore, unpaired substrate regions can exert a rather complex influence on the overall activity of DED1, and consequently, the context of a given substrate

even outside of a duplex region may potentially impact RNA rearrangements by DED1.

The ability to remodel RNA structures through more than duplex unwinding expands the horizon for possible roles of DED1 (and other related DEAD-box proteins) beyond the disruption of RNA−RNA or RNA−protein interactions. Although the physiological significance of combined unwinding and annealing activities has not been specifically explored for DED1 or other DEAD-box proteins, DED1 is one of the most efficient enzymes to catalyze strand annealing. This profound activity is thus worth considering when envisioning potential biological functions of DED1, an essential protein in yeast. In this context, it is notable (i) that deletion of the 90 C-terminal amino acids of DED1, which are shown here to enhance the annealing activity of DED1, is lethal in *S. cerevisiae* (T. H. Chang, personal communication) and (ii) that the *S. pombe* DED1 homologue was identified in a screen for factors promoting antisense-mediated gene silencing (*22*). We emphasize that there are clearly alternative explanations for these two observations; however, a strand annealing activity of DED1 would directly account for those results.

Although the exact physiological targets of DED1 are currently unknown, it is attractive to speculate that the enzyme may use its two opposing activities to directly facilitate ATP-dependent exchanges of RNA−RNA or protein−RNA interactions. ATP-driven exchanges of mutually exclusive RNA−RNA interactions as well as protein−RNA exchanges are well documented in mRNA splicing or ribosome biogenesis (*23*), and DED1 (and p68, which also anneals RNA strands *(7)*) has been found in both spliceosomal and ribosomal precursor particles (*24*, *25*).

Nonetheless, proximity of RNA helicase and strand annealing activities have been observed to date only for separate proteins. For instance, the DEAD-box protein eIF4A interacts with eIF4B, which catalyzes strand annealing in vitro, and the DExH protein Brr2 functions in conjunction with Prp24, which promotes annealing of RNAs (*26*−*28*). A protein harboring both ATP-dependent unwinding and strand annealing activities would be well-suited to perform more complex remodeling reactions without the simultaneous need for multiple protein factors. It is also important to note that the intermolecular strand annealing activities shown for DED1, p68, and other DEAD-box proteins may be relevant for intramolecular duplex formation, that is, RNA folding, as recently shown for the DEAD-box protein RH-II/Gu (*29*).

Besides the mechanistic possibilities afforded by DEAD-box proteins that promote both strand annealing and disruption of RNA−RNA or RNA−protein interactions, the regulation of the two opposing activities is of potential biological importance. Because the balance between unwinding and annealing activities is sensitive to ATP and ADP concentrations, it is conceivable that DED1 utilizes such ATP and/or ADP modulation in one or more of its myriad physiological roles (*8*). In fact, the maximal modulation by ADP under our reaction conditions occurs in the range of physiological ADP/ATP ratios (*30*). It is thus possible that DED1 adjusts its activity under metabolic stress situations that are accompanied by changes in ADP and/or ATP concentrations.

Finally, the remarkably distinct response of DED1 to different RNA substrates could conceivably provide a physiological advantage. The ability to differentially remodel distinct RNA substrates could reflect the adaptation of DED1 to its multiple biological functions in pre-mRNA splicing, RNA export, and translation initiation, where the enzyme has been shown to be required for the regulation of specific genes (*8*, *31*).

Collectively, our observations have added an intriguing facet to the known mechanistic repertoire of the ubiquitous DEAD-box protein family. The ability to balance strand annealing and duplex unwinding in a dynamic and ATP/ADP-dependent fashion raises the question whether a subset of DEAD-box proteins including DED1 and p68 might be more appropriately considered "RNA remodelers", rather than "just" RNA helicases or RNPases. It will now be interesting to understand mechanistic implications of ATP and ADP "tunable" RNA unwinding and strand annealing activities combined in a single enzyme. At the same time, it will be critical to elucidate physiological ramifications of concurrent unwinding and annealing activities in the growing number of DEAD-box proteins that catalyze both strand separation and duplex formation.

ACKNOWLEDGMENT

We thank Wen Wang for help with the construction and purification of $DED1_{\Delta C}$ and Dr. W. C. Merrick for the gift of purified eIF4A. We thank Anna Marie Pyle, Tim Nilsen, Vernon Anderson, Peter deHaseth, and members of our laboratory for comments on the manuscript. E.J. is a Scholar of the Damon Runyon Cancer Research Foundation.

REFERENCES

1. Rocak, S., and Linder, P. (2004) DEAD-box proteins: the driving forces behind RNA metabolism, *Nat. Rev. Mol. Cell Biol. 5*, 232−241.
2. Tanner, N. K., and Linder, P. (2001) DExD/H box RNA helicases. From generic motors to specific dissociation functions, *Mol. Cell 8*, 251−261.
3. Anantharaman, V., Koonin, E. V., and Aravind, L. (2002) Comparative genomics and evolution of proteins involved in RNA metabolism, *Nucleic Acids Res. 30*, 1427−1464.
4. Schwer, B. (2001) A new twist on RNA helicases: DExH/D box proteins as RNPases, *Nat. Struct. Biol. 8*, 113−116.
5. Fairman, M., Maroney, P. A., Wang, W., Bowers, H., Gollnick, P., Nilsen, T. W., and Jankowsky, E. (2004) Protein displacement by DExH/D RNA helicases without duplex unwinding, *Science 304*, 730−734.
6. Chamot, D., Colvin, K. R., Kujat-Choy, S. L., and Owttrim, G. W. (2005) RNA structural rearrangement via unwinding and annealing by the cyanobacterial RNA helicase, CrhR, *J. Biol. Chem. 280*, 2036−2044.
7. Rossler, O. G., Straka, A., and Stahl, H. (2001) Rearrangement of structured RNA via branch migration structures catalysed by the highly related DEAD-box proteins p68 and p72, *Nucleic Acids Res. 29*, 2088−2096.
8. Linder, P. (2003) Yeast RNA helicases of the DEAD-box family involved in translation initiation, *Biol. Cell 95*, 157−167.
9. Iost, I., Dreyfus, M., and Linder, P. (1999) Ded1p, a DEAD-box protein required for translation initiation in *Saccharomyces cerevisiae*, is an RNA helicase, *J. Biol. Chem. 274*, 17677−17683.
10. Jankowsky, E., Gross, C. H., Shuman, S., and Pyle, A. M. (2000) The DExH protein NPH-II is a processive and directional motor for unwinding RNA, *Nature 403*, 447−451.
11. Rogers, G. W., Richter, N. J., and Merrick, W. C. (1999) Biochemical and kinetic characterization of the RNA helicase activity of eukaryotic initiation factor 4A, *J. Biol. Chem. 274*, 12236−12244.

12. Jankowsky, E., Gross, C. H., Shuman, S., and Pyle, A. M. (2001) Active disruption of an RNA−protein interaction by a DExH/D RNA helicase, *Science 291*, 121−125.
13. Berg, O. G., and von Hippel, P. H. (1985) Diffusion-controlled macromolecular interactions, *Annu. Rev. Biophys. Biophys. Chem. 14*, 131−160.
14. Urbaneja, M. A., Wu, M., Casas-Finet, J. R., and Karpel, R. L. (2002) HIV-1 nucleocapsid protein as a nucleic acid chaperone: spectroscopic study of its helix-destabilizing properties, structural binding specificity, and annealing activity, *J. Mol. Biol. 318*, 749−764.
15. Nedbal, W., Frey, M., Willemann, B., Zentgraf, H., and Sczakiel, G. (1997) Mechanistic insights into p53-promoted RNA−RNA annealing, *J. Mol. Biol. 266*, 677−687.
16. Muller, U. F., Lambert, L., and Goringer, H. U. (2001) Annealing of RNA editing substrates facilitated by guide RNA-binding protein gBP21, *EMBO J. 20*, 1394−1404.
17. Kim, J. L., Morgenstern, K. A., Griffith, J. P., Dwyer, M. D., Thomson, J. A., Murcko, M. A., Lin, C., and Caron, P. R. (1998) Hepatitis C virus NS3 RNA helicase domain with a bound oligonucleotide: the crystal structure provides insights into the mode of unwinding, *Structure 6*, 89−100.
18. Pontius, B. W., and Berg, P. (1990) Renaturation of complementary DNA strands mediated by purified mammalian heterogeneous nuclear ribonucleoprotein A1 protein: implications for a mechanism for rapid molecular assembly, *Proc. Natl. Acad. Sci. U.S.A. 87*, 8403−8407.
19. Draper, D. E. (1999) Themes in RNA−protein recognition, *J. Mol. Biol. 293*, 255−270.
20. Willamson, J. R. (2000) Induced fit in RNA−protein recognition, *Nat. Struct. Biol. 7*, 834−837.
21. Cristofari, G., and Darlix, J. L. (2002) The ubiquitous nature of RNA chaperone proteins, *Prog. Nucleic Acid Res. Mol. Biol. 72*, 223−268.
22. Raponi, M., and Arndt, G. M. (2002) Dominant genetic screen for cofactors that enhance antisense RNA-mediated gene silencing in fission yeast, *Nucleic Acids Res. 30*, 2546−2554.
23. Staley, J. P., and Guthrie, C. (1998) Mechanical devices of the spliceosome: motors, clocks, springs, and things, *Cell 92*, 315−326.
24. Schafer, T., Strauss, D., Petfalski, E., Tollervey, D., and Hurt, E. (2003) The path from nucleolar 90S to cytoplasmic 40S pre-ribosomes, *EMBO J. 22*, 1370−1380.
25. Stevens, S. W., Ryan, D. E., Ge, H. Y., Moore, R. E., Young, M. K., Lee, T. D., and Abelson, J. (2002) Composition and functional characterization of the yeast spliceosomal penta-snRNP, *Mol. Cell 9*, 31−44.
26. Raghunathan, P. L., and Guthrie, C. (1998) RNA unwinding in U4/U6 snRNPs requires ATP hydrolysis and the DEIH-box splicing factor Brr2, *Curr. Biol 8*, 847−855.
27. Altmann, M., Wittmer, B., Methot, N., Sonenberg, N., and Trachsel, H. (1995) The *Saccharomyces cerevisiae* translation initiation factor Tif3 and its mammalian homologue, eIF-4B, have RNA annealing activity, *EMBO J. 14*, 3820−3827.
28. Niederberger, N., Trachsel, H., and Altmann, M. (1998) The RNA recognition motif of yeast translation initiation factor Tif3/eIF4B is required but not sufficient for RNA strand-exchange and translational activity, *RNA 4*, 1259−1267.
29. Valdez, B. C. (2000) Structural domains involved in the RNA folding activity of RNA helicase II/Gu protein, *Eur. J. Biochem. 267*, 6395−6402.
30. Larsson, C., Pahlman, I. L., and Gustafsson, L. (2000) The importance of ATP as a regulator of glycolytic flux in *Saccharomyces cerevisiae*, *Yeast 16*, 797−809.
31. Burckin, T., Nagel, R., Mandel-Gutfreund, Y., Shiue, L., Clark, T. A., Chong, J. L., Chang, T. H., Squazzo, S., Hartzog, G., and Ares, M. J. (2005) Exploring functional relationships between components of the gene expression machinery, *Nat. Struct. Mol. Biol. 12*, 175−182.
32. Jeanmougin, F., Thompson, J. D., Gouy, M., Higgins, D. G., and Gibson, T. J. (1998) Multiple sequence alignment with Clustal X, *Trends Biochem. Sci. 23*, 403−405.

BI0508946